NORGES TEKNISK-NATURVITENSKAPELIGE
UNIVERSITET

A high order splitting method for time-dependent domains

by

Tormod Bjøntegaard and Einar M. Rønquist

PREPRINT
NUMERICS NO. 1/2008

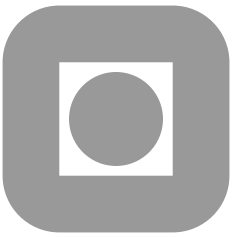

NORWEGIAN UNIVERSITY OF
SCIENCE AND TECHNOLOGY
TRONDHEIM, NORWAY

This report has URL
http://www.math.ntnu.no/preprint/numerics/2008/N1-2008.pdf
Address: Department of Mathematical Sciences, Norwegian University of Science and Technology, N-7491 Trondheim, Norway.

A high order splitting method for time-dependent domains

Tormod Bjøntegaard and Einar M. Rønquist

March 31, 2008

We present a temporal splitting scheme for the semi-discrete convection-diffusion equation and the semi-discrete incompressible Navier-Stokes equations in time-depedent geometries. The proposed splitting scheme can be considered as an extension of the OIF-method proposed in [22] in the sense that it can be interpreted as a semi-Lagrangian method for time-dependent domains. The semi-discrete equations are derived from an arbitrary Lagrangian-Eulerian (ALE) formulation of the governing equations, and are discretized in space using high order spectral elements. The proposed splitting scheme has been tested numerically on model problems with known analytical solutions, and first, second, and third order convergence in time has been obtained. We also show that it is not necessary for the interior mesh velocity to be obtained through the use of an elliptic solver. Numerical tests show that it is sufficient that the mesh velocity is regular within each spectral element and only C^0-continuous across element boundaries; this is consistent with the theoretical results presented in [9]. In addition, the mesh velocity should be regular in the time direction.

Keywords: Time-dependent domains; ALE-formulation; operator splitting; spectral elements

1 Introduction

Numerical solution of the Navier-Stokes equations in time-dependent geometries has found wide-spread use in science and engineering, both in the context of basic understanding of fluid flow phenomena, as well as for predictive purposes in engineering. A powerful framework is provided by the arbitrary Lagrangian-Eulerian (ALE) formulation [13, 16, 6, 15]. Even though this framework is quite mature and is currently used in many commercial codes, it is still a subject of active research; e.g., see [15].

Part of the current research in ALE methods is related to time integration. One issue is the importance of satisfying the so-called geometric conservation law [18, 12, 10, 7]. The conclusion is not quite clear for general Navier-Stokes problems. One complicating factor in all this effort is the fact that it is not easy to measure and verify the overall temporal accuracy during a transient simulation. This is partially due to the lack of analytical solutions for moving boundary problems, in particular, for general free surface problems where both normal and tangential stress boundary conditions are imposed.

The evolution of the surface of a time-dependent domain is typically determined via a kinematic condition which says that the normal domain velocity must coincide with

the normal fluid velocity along the surface. Assuming that this surface evolution can be tracked in an accurate and efficient way, it still remains to extend the surface deformation to the interior of the domain. A smooth extension of the mesh velocity to the interior is most commonly used, e.g., using an harmonic extension, a Stokes solver, or an elasticity solver. However, other possible choices do not seem to have been fully explored; see [9] for a theoretical discussion of this issue.

The purpose of this paper is to present recent results on developing high order splitting methods for problems in time-dependent domains. Our long term goal is to be able to study large-scale free surface applications like three-dimensional Bénard-Marangoni convection including deformed surfaces [3], or problems involving fluids enclosed in flexible membranes on much larger length scales than typically associated with surface-tension-dominated effects. The latter problem is motivated by the transportation of fresh water using elastic fabric containers; see [19, 2].

In Section 2, we first present the governing equations for incompressible fluid flow and heat transfer problem in time-dependent domains. The ALE-formulation presented in Section 3 is the natural point of departure for the spatial discretization. In Section 4, we present a set of semi-discrete equations based on the spectral element method, however, any finite element method can in principle be used for the spatial discretization.

In Section 5, we present an operator splitting method for the temporal treatment of the convection-diffusion problem. The approach represents an extension of the OIF-method proposed in [22] to time-dependent domains. We conclude this section by showing numerical results for a two-dimensional test problem involving a moving front.

In Section 6, we discuss the proposed splitting scheme in the context of solving incompressible fluid flow problems. The splitting scheme represents a convection-Stokes splitting, which can also be interpreted as a semi-Lagrangian scheme. We present numerical evidence of first, second, and third order convergence in time for a three-dimensional ALE test problem with a known analytical solution. The issue of global regularity requirement for the mesh velocity is also illuminated.

In Section 7, we conclude our study and comment on future extensions.

2 Governing equations: strong form

In the following we consider the numerical solution of unsteady fluid flow and heat transfer problems in time-dependent domains. Specifically, we consider the incompressible Navier-Stokes equations and the convection-diffusion equation in a domain $\Omega(t)$,

$$\frac{\partial u_j}{\partial x_j} = 0, \qquad \text{in } \Omega(t), \tag{1}$$

$$\rho\left(\frac{\partial u_i}{\partial t} + u_j\frac{\partial u_i}{\partial x_j}\right) = \frac{\partial \sigma_{ij}}{\partial x_j} + f_i, \qquad \text{in } \Omega(t), \qquad i = 1,2,3, \tag{2}$$

$$\rho\, c_p\left(\frac{\partial \Theta}{\partial t} + u_j\frac{\partial \Theta}{\partial x_j}\right) = k\,\frac{\partial^2 \Theta}{\partial x_j \partial x_j} + g, \qquad \text{in } \Omega(t). \tag{3}$$

In (1) and (2), u_i is the i-th component of the fluid velocity in an inertial reference frame, x_j is the j-th coordinate, f_i is the i-th component of a volumetric body force, and ρ is the density of the fluid. Summation over repeated indices is assumed. The stress tensor σ_{ij} is

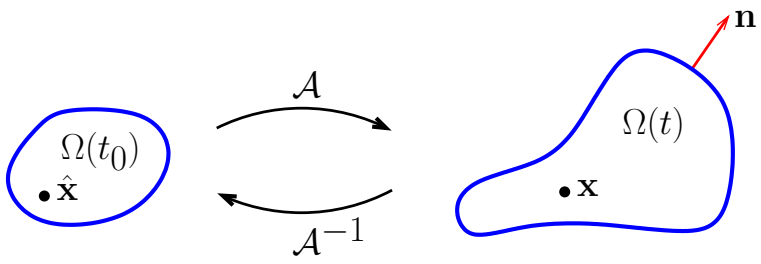

Figure 1: The time-dependent domain $\Omega(t)$ can be regarded as a one-to-one mapping $\mathcal{A}$ of a reference configuration $\Omega(t_0)$. The outward unit normal vector along $\partial\Omega(t)$ is denoted as $\mathbf{n}$.

here given as

$$\sigma_{ij} = -p\delta_{ij} + \mu\left(\frac{\partial u_i}{\partial x_j} + \frac{\partial u_j}{\partial x_i}\right), \qquad i,j = 1,2,3, \tag{4}$$

where p is the pressure, μ is the dynamic viscosity, and δ_{ij} is the Kronecker delta symbol. In (3), Θ is the temperature, c_p is the specific heat capacity, k is the thermal conductivity, and g is a volumetric heat source.

We consider here the stress formulation for incompressible fluid flow because our intended use of the proposed splitting scheme is to be able to accurately simulate time-dependent free surface flows with very general boundary conditions (including thermo-capillary effects). The particular boundary conditions used in the numerical tests in this paper will be discussed later.

3 ALE-formulation

In this section we briefly discuss the governing equations for fluid flow and heat transfer in time-dependent domains. In particular, we follow the arbitrary Lagrangian-Eulerian (ALE) framework which represents a powerful starting point for the numerical approximation of such problems [13, 16, 6, 15].

One of the key ingredients in the ALE-framework is the introduction of a domain velocity $\mathbf{w}$. Following closely the notation of [10] and [5], we can regard the time-dependent domain $\Omega(t)$ as a mapping $\mathcal{A}$ of a reference configuration $\Omega(t_0)$, e.g., the domain at an earlier time t_0; see Figure 1. We assume that $\mathcal{A}$ is a continuous and one-to-one mapping, i.e., a unique point $\hat{\mathbf{x}}$ in $\Omega(t_0)$ maps to a unique point $\mathbf{x}$ in $\Omega(t)$,

$$\begin{aligned} &\mathcal{A} \in C^0(\overline{\Omega(t_0)}, t), \\ &\mathbf{x} = \mathcal{A}(\hat{\mathbf{x}}, t). \end{aligned}$$

In particular,

$$\partial\Omega(t) = \mathcal{A}(\partial\Omega(t_0), t).$$

The domain velocity $\mathbf{w}$ at a point $\mathbf{x}$, corresponding to a particular location $\hat{\mathbf{x}}$ in the reference configuration, can then be defined as

$$\mathbf{w} = \left(\frac{\partial \mathcal{A}}{\partial t}\right)\Big|_{\hat{\mathbf{x}}} \circ \mathcal{A}^{-1}(\mathbf{x}, t).$$

If $\mathbf{u}$ represents the fluid velocity in $\Omega(t)$, it follows from the continuum hypothesis that

$$\mathbf{w} \cdot \mathbf{n} = \mathbf{u} \cdot \mathbf{n} \quad \text{along } \partial\Omega(t). \tag{5}$$

The condition (5) is called the kinematic condition.

The ALE-formulation can be derived from the weak form of the governing equations using an Eulerian framework, and then apply the Reynolds' transport theorem and Euler's expansion formula [1]. Following this approach, the ALE-formulation of the heat transfer problem can be expressed as: Find Θ (the temperature) $\in X \subset H^1(\Omega)$ such that

$$\frac{\mathrm{d}}{\mathrm{d}t}(v,\Theta) + c(v,\Theta) - e(v,\Theta) = -a_\Theta(v,\Theta) + (v,g) + \ell_\Theta(v), \qquad \forall v \in X, \tag{6}$$

where we have defined the following bilinear forms,

$$(v,\phi) = \int_{\Omega(t)} v\phi \ \mathrm{d}V, \tag{7}$$

$$c(v,\phi) = \int_{\Omega(t)} v(u_j - w_j)\frac{\partial \phi}{\partial x_j} \ \mathrm{d}V, \tag{8}$$

$$e(v,\phi) = \int_{\Omega(t)} v\phi\frac{\partial w_j}{\partial x_j} \, \mathrm{d}V, \tag{9}$$

$$a_\Theta(v,\phi) = \int_{\Omega(t)} k \, \frac{\partial v}{\partial x_j}\frac{\partial \phi}{\partial x_j} \, \mathrm{d}V, \tag{10}$$

as well as the linear form

$$\ell_\Theta(v) = \int_{\partial\Omega(t)} v\frac{\partial \Theta}{\partial n} \, \mathrm{d}S. \tag{11}$$

With no loss in generality, we have set ρc_p equal to unity, and we have assumed homogeneous Dirichlet boundary conditions for Θ along part of, or all of, the boundary $\partial\Omega(t)$.

One advantage with the form (6) is that the time-derivative appears outside the integral over $\Omega(t)$; this will prove very useful for the subsequent numerical treatment. Second, the contribution from convection appears in two terms: a standard convection term where a relative convection velocity $(\mathbf{u} - \mathbf{w})$ appears (see (8)), as well as an "expansion" term involving the divergence of the domain velocity (see (9)). The first term on the right hand side represents the standard diffusion term resulting from integration by parts, while the third term represents the associated surface term allowing for a convenient imposition of flux boundary conditions; as usual, this term vanishes wherever essential boundary conditions are prescribed. The second term on the right hand side represents a prescribed heat source (which we assume is square integrable).

A similar procedure for the fluid problem yields the ALE-formulation of the incompressible Navier-Stokes equations: find $\mathbf{u} \in X \subset (H^1(\Omega))^3$ and $p \in Y \subset L^2(\Omega)$ such that

$$\frac{\mathrm{d}}{\mathrm{d}t}(\mathbf{v},\mathbf{u}) + c(\mathbf{v},\mathbf{u}) - e(\mathbf{v},\mathbf{u}) = -a_\sigma(\mathbf{v},\mathbf{u}) + d(p,\mathbf{v}) + (\mathbf{v},\mathbf{f}) + \ell_\sigma(\mathbf{v}), \qquad \forall \mathbf{v} \in X, \tag{12}$$

$$d(q,\mathbf{u}) = 0, \qquad \forall q \in Y, \tag{13}$$

where we have introduced the bilinear forms

$$(\mathbf{v}, \mathbf{u}) = \int_{\Omega(t)} v_i u_i \, \mathrm{d}V, \tag{14}$$

$$c(\mathbf{v}, \mathbf{u}) = \int_{\Omega(t)} v_i (u_j - w_j) \frac{\partial u_i}{\partial x_j} \, \mathrm{d}V, \tag{15}$$

$$e(\mathbf{v}, \mathbf{u}) = \int_{\Omega(t)} v_i u_i \frac{\partial w_j}{\partial x_j} \, \mathrm{d}V, \tag{16}$$

$$a_\sigma(\mathbf{v}, \mathbf{u}) = \int_{\Omega(t)} \mu \, \frac{\partial v_i}{\partial x_j} \left(\frac{\partial u_i}{\partial x_j} + \frac{\partial u_j}{\partial x_i} \right) \mathrm{d}V, \tag{17}$$

$$d(q, \mathbf{u}) = \int_{\Omega(t)} q \frac{\partial u_j}{\partial x_j} \, \mathrm{d}V, \tag{18}$$

as well as the linear form

$$\ell_\sigma(v) = \int_{\partial\Omega(t)} v_i \sigma_{ij} n_j \, \mathrm{d}S. \tag{19}$$

With no loss in generality, we have here set ρ equal to unity. In the above definitions of the bilinear and linear forms, summation over repeated indices is assumed. Similar to the heat transfer problem, we have assumed homogeneous Dirichlet boundary conditions for the velocity $\mathbf{u}$ along part of, or all of, the boundary $\partial\Omega(t)$.

The linear form (19) follows from integration by parts of the term $\int_{\Omega(t)} v_i \frac{\partial \sigma_{ij}}{\partial x_j} \, \mathrm{d}V$; this surface term allows for a convenient imposition of stress boundary conditons (both normal and tangential), while the surface term vanishes wherever essential velocity boundary conditions are prescribed.

4 Semi-discrete problem

The weak form presented above will be our point of departure for the spatial and temporal discretization. Our goal is to achieve high order accuracy both in the space and time. We start with a brief discussion of the spatial discretization which will be based on spectral elements [21]. Following this approach, we decompose the domain into disjoint elements and approximate all the field variables as high-order polynomials within each element. Appropriate C^0-continuity conditions are imposed across interelement boundaries for second-order problems as considered here. We assume that a high-order, tensor-product nodal basis is used. Following this approach, we arrive at a system of semi-discrete equations for the heat transfer problem (6) on the form

$$\frac{\mathrm{d}}{\mathrm{d}t}(\underline{\mathbf{B}}\,\underline{\Theta}) + \underline{\mathbf{C}}\,\underline{\Theta} = -\underline{\mathbf{A}}\,\underline{\Theta} + \underline{\mathbf{E}}\,\underline{\Theta} + \underline{\mathrm{b}}, \tag{20}$$

$$\frac{\mathrm{d}\underline{\mathbf{x}}}{\mathrm{d}t} = \underline{\mathbf{w}}. \tag{21}$$

Equation (20) represents the semi-discrete convection-diffusion equation derived from the ALE-formulation, while equation (21) represents the system of ordinary differential equations governing the mesh evolution. All the lower case symbols represent vectors of nodal values at a particular time: $\underline{\Theta}$ represents the temperature, $\underline{\mathbf{x}}$ represents the coordinates of the grid points, $\underline{\mathbf{u}}$ and $\underline{\mathbf{w}}$ represent the fluid velocity and mesh velocity, respectively, and $\underline{\mathrm{b}}$ represents the known data (source term and boundary conditions). Furthermore, $\underline{\mathbf{B}}$ represents the time-dependent mass matrix derived from (7), which in our case is diagonal because of the fact that the quadrature points and nodal points that we use within each spectral element coincide [21]. The matrix $\underline{\mathbf{A}}$ represents the discrete Laplacian derived from (10), which is time-dependent because the computational domain is time-dependent. The matrix $\underline{\mathbf{C}}$ represents the convection operator derived from (8); this will again depend on time through the time-dependent computational domain, but also via the fluid velocity $\underline{\mathbf{u}}$ and the mesh velocity $\underline{\mathbf{w}}$. Finally, the matrix $\underline{\mathbf{E}}$ represents the discrete "expansion" term associated with the bilinear form (9).

In a similar way we can derive a set of semi-discrete equations for the incompressible fluid flow problem (12)-(13); these equations can be expressed as

$$\frac{\mathrm{d}}{\mathrm{d}t}(\underline{\mathbf{B}}\,\underline{\mathbf{u}}) + \underline{\mathbf{C}}\,\underline{\mathbf{u}} = -\underline{\mathbf{A}}_\sigma\,\underline{\mathbf{u}} + \underline{\mathbf{D}}^T\underline{p} + \underline{\mathbf{E}}\,\underline{\mathbf{u}} + \underline{\mathbf{b}}, \tag{22}$$

$$\underline{\mathbf{D}}\,\underline{\mathbf{u}} = \underline{0}, \tag{23}$$

$$\frac{\mathrm{d}\underline{\mathbf{x}}}{\mathrm{d}t} = \underline{\mathbf{w}}. \tag{24}$$

Here, $\underline{\mathbf{B}}$ represents the time-dependent mass matrix derived from (14) (i.e., for the vector case), $\underline{\mathbf{C}}$ represents the time-dependent convection operator derived from (15) (which is now nonlinear and couples all the velocity components), $\underline{\mathbf{A}}_\sigma$ represents the symmetric, viscous operator derived from (17) (which couples all the velocity components), $\underline{\mathbf{D}}$ represents the discrete divergence operator derived from (18), while $\underline{\mathbf{D}}^T$ is the corresponding discrete gradient operator, $\underline{\mathbf{E}}$ represents the discrete "expansion" operator derived from (16) (i.e., for the vector case), and $\underline{\mathbf{b}}$ is a known right hand side derived from (14) and (19).

We remark that other finite-element-based discretization methods could also have been used for the spatial discretization; the resulting semi-discrete equations could still be expressed on the form (20)-(21), or (22)-(24), and thus the following discussion regarding the temporal treatment also applies to such discretizations.

5 A convection-diffusion splitting scheme

Our goal is here to propose a high order temporal splitting scheme for (20)-(21); with high order we shall here mean higher than first order, in particular, second and third order convergence in time. Our point of departure will be the Operator-Integration-Factor (OIF) procedure proposed in [22]. The computational approach we propose in this paper can be viewed as an extension of the OIF-method to time-dependent domains.

5.1 Fixed domain

Before we discuss the details of the new scheme, let us first revisit some aspects of the original OIF-approach applied to the convection-diffusion problem. First, we assume a fixed domain Ω. Following a standard Eulerian description, the semi-discrete equations for the convection-diffusion problem can be expressed as

$$\underline{\mathbf{B}}\,\frac{\mathrm{d}\underline{\Theta}}{\mathrm{d}t} + \underline{\mathbf{C}}\,\underline{\Theta} = -\underline{\mathbf{A}}\,\underline{\Theta} + \underline{\mathrm{b}}, \tag{25}$$

where now all the discrete spatial operators are time-independent. Although the OIF-method presented in [22]Ê offers a quite general framework for deriving temporal splitting methods, this method applied to the particular convection-diffusion problem (25) can also be interpreted as a particular semi-Lagrangian method. Specifically, a first order splitting scheme reads

$$\underline{\mathbf{B}} \left(\frac{\underline{\Theta}^{n+1} - \widetilde{\underline{\Theta}}^{n+1}}{\Delta t} \right) = -\underline{\mathbf{A}}\, \underline{\Theta}^{n+1} + \underline{\mathrm{b}}^{n+1}, \tag{26}$$

where the expression inside the parentheses on the left hand side represents a first order approximation to the total derivative $\mathrm{D}\Theta/\mathrm{D}t$ at time t^{n+1}. With this interpretation $\widetilde{\underline{\Theta}}^{n+1}$ represents the values of Θ at time t^n for those fluid particles which at time t^{n+1} coincide with the *fixed* grid points used in a pure Eulerian formulation; note that the position these fluid particles had at time t^n do *not* coincide with the grid points.

An attractive aspect with the OIF-method is the fact that it is possible to find the values $\widetilde{\underline{\Theta}}^{n+1}$ only by using information at the fixed grid points. This is in contrast to other semi-Lagrangian schemes where the positions of the fluid particles at earlier times first have to be computed by following the characteristics backwards in time, and then the solution at an earlier time needs to be interpolated at these points; see [23, 11]. In the OIF-method [22], however, the values $\widetilde{\underline{\Theta}}^{n+1}$ are found by solving the following pure convection problem defined in the interval t^n to t^{n+1},

$$\underline{\mathbf{B}}\, \frac{\mathrm{d}\widetilde{\underline{\Theta}}}{\mathrm{d}t} = -\underline{\mathbf{C}}\, \widetilde{\underline{\Theta}}, \qquad \widetilde{\underline{\Theta}}^{n} = \underline{\Theta}^{n}, \qquad t^n \le t \le t^{n+1}. \tag{27}$$

In essence, the values $\widetilde{\underline{\Theta}}^{n+1}$ we are interested in are being convected to the fixed grid points through the solution of (27).

The extension to second order in time is quite natural. We now use a second-order (Backward Differentiation) approximation of the total derivative $\mathrm{D}\Theta/\mathrm{D}t$ at time t^{n+1},

$$\underline{\mathbf{B}} \left(\frac{\frac{3}{2}\underline{\Theta}^{n+1} - 2\widetilde{\underline{\Theta}}^{n+1} + \frac{1}{2}\widetilde{\widetilde{\underline{\Theta}}}^{n+1}}{\Delta t} \right) = -\underline{\mathbf{A}}\, \underline{\Theta}^{n+1} + \underline{\mathrm{b}}^{n+1}. \tag{28}$$

The values of Θ at times t^n and t^{n-1} for those fluid particles which at time t^{n+1} coincide with the fixed grid points are now found by solving the two pure convection problems

$$\underline{\mathbf{B}}\, \frac{\mathrm{d}\widetilde{\underline{\Theta}}}{\mathrm{d}t} = -\underline{\mathbf{C}}\, \widetilde{\underline{\Theta}}, \qquad \widetilde{\underline{\Theta}}^{n} = \underline{\Theta}^{n}, \qquad t^n \le t \le t^{n+1}, \tag{29}$$

$$\underline{\mathbf{B}}\, \frac{\mathrm{d}\widetilde{\widetilde{\underline{\Theta}}}}{\mathrm{d}t} = -\underline{\mathbf{C}}\, \widetilde{\widetilde{\underline{\Theta}}}, \qquad \widetilde{\widetilde{\underline{\Theta}}}^{n-1} = \underline{\Theta}^{n-1}, \qquad t^{n-1} \le t \le t^{n+1}. \tag{30}$$

We now discuss the temporal discretization of the pure convection problems defined above. First, the discrete convection operator $\underline{\mathbf{C}}$ depends on the given convection velocity. In practice, this velocity field is typically coming from a Navier-Stokes solver and is only known at discrete times t^n, t^{n-1}, etc. We therefore approximate the convection velocity in time by using a polynomial interpolant/extrapolant. Specifically, for a first order approximation, see (26) and (27), the convection velocity is set equal to $\underline{\mathbf{u}}^n$ for the entire time interval $t^n \le t \le t^{n+1}$ in (27). For a second order approximation, the convection velocity used in (29) and (30) is approximated linearly between t^{n-1} and t^{n+1}; see Figure 2.

In order to solve the single initial value problem (27), or the two initial value problems (29) and (30), we use the classical fourth order explicit Runge-Kutta scheme (ERK4).

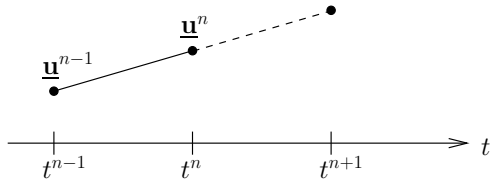

Figure 2: The convecting velocity field is approximated linearly in time in the interval $[t^{n-1}, t^{n+1}]$ for a second order OIF-scheme. In particular, the convecting velocity field is constructed as the linear interpolant between t^{n-1} and t^n, and as the linear extrapolant between t^n and t^{n+1}.

An explicit scheme avoids the need to solve non-symmetric (and in the case of solving the Navier-Stokes equations, nonlinear) equation systems. Second, the ERK4 scheme is attractive to use since it is accurate and the associated stability region encloses a significant part of the imaginary axis. The time step used for these "inner" convection problems can be the same as for the "outer" diffusion problem, however, this is not a requirement. On the other hand, we are required to honor the Courant stability criterion and we also need to honor a final integration time equal to t^{n+1}.

Finally, we mention that the OIF-approach presented above may also be extended to third order in time. In this case, we use a third order Backward Differentiation approximation of the total derivative, and we need to solve three separate convection problems. Furthermore, the given convection field is now constructed as a second order interpolant/extrapolant in the interval between t^{n-2} and t^{n+1}.

5.2 Time-dependent domain

We now consider the extension of the OIF-approach to time-dependent domains. In particular, we consider the solution of (20) and (21). As mentioned earlier, all the discrete spatial operators are now time-dependent.

In order to more easily apply the OIF formalism to this problem, we first define the new variable

$$\underline{\Phi} = \underline{\mathbf{B}}\,\underline{\Theta}. \tag{31}$$

The convection-diffusion equation (20) can then be expressed as

$$\frac{\mathrm{d}\underline{\Phi}}{\mathrm{d}t} + \underline{\mathbf{C}}\,\underline{\mathbf{B}}^{-1}\underline{\Phi} = -(\underline{\mathbf{A}} - \underline{\mathbf{E}})\,\underline{\mathbf{B}}^{-1}\underline{\Phi} + \underline{\mathrm{b}}. \tag{32}$$

Next, we apply the OIF-method to the system (32). Treating the expansion term as part of the "outer" problem, a first order splitting scheme can be expressed as

$$\left(\frac{\underline{\mathbf{B}}^{n+1}\underline{\Theta}^{n+1} - \widetilde{\underline{\Phi}}^{n+1}}{\Delta t}\right) = -(\underline{\mathbf{A}}^{n+1} - \underline{\mathbf{E}}^{n+1})\,\underline{\Theta}^{n+1} + \underline{\mathrm{b}}^{n+1}. \tag{33}$$

The values $\widetilde{\underline{\Phi}}^{n+1}$ are obtained through the solution of the following ("inner") convection problem,

$$\frac{\mathrm{d}\widetilde{\underline{\Phi}}}{\mathrm{d}t} = -\underline{\mathbf{C}}\,\underline{\mathbf{B}}^{-1}\,\widetilde{\underline{\Phi}}, \qquad \widetilde{\underline{\Phi}}^{n} = \underline{\mathbf{B}}^{n}\underline{\Theta}^{n}, \qquad t^n \le t \le t^{n+1}. \tag{34}$$

Finally, we solve the system (21) using an explicit multi-step scheme; for a first order approximation in time, we simply use a first order Adams-Bashforth scheme (i.e, Euler Forward),

$$\left(\frac{\underline{\mathbf{x}}^{n+1} - \underline{\mathbf{x}}^{n}}{\Delta t}\right) = \underline{\mathbf{w}}^{n}. \tag{35}$$

We now make a few remarks concerning this splitting scheme. Similar to the standard OIF-scheme for fixed domains, we use a Backward-Differentiation (BD) scheme for the "outer" problem. This is mainly due to the convenience of only having to evaluate all the associated operators on the right hand side at time level t^{n+1}. The associated "Operator Integrating Factor" is defined to be the identity operator at t^{n+1} [22], and the use of a BD-scheme thus avoids having to solve additional "inner" problems.

Second, we note that the introduction of the new variable Φ in (31) necessitates a modified "inner" convection problem in (34) compared to the corresponding problem (27) for time-independent domains. This modification is necessary due to the fact that the mass matrix is time-dependent.

Third, the discrete operator $\underline{\mathbf{C}}\,\underline{\mathbf{B}}^{-1}$ in (34) depends on the convecting velocity field $\mathbf{u}$, on the mesh velocity $\mathbf{w}$, and on the computational domain Ω. All these quantities are approximated as constants, and equal to the the corresponding values at time t^n for a first order splitting scheme.

Fourth, similar to the system (27), the system (34) is solved using ERK4. An important observation here is the following. In the ALE formulation the convection operator $\underline{\mathbf{C}}$ is derived from the associated bilinear form (8). This form includes an "effective" convection velocity $\mathbf{u} - \mathbf{w}$. However, using integration-by-parts, we can easily show that this form is skew-symmetric, i.e.,

$$c(v, \phi) = -c(\phi, v). \tag{36}$$

This follows by noticing that the boundary integral over $\partial\Omega$ vanishes either due to essential boundary conditions or due to the kinematic condition (5). Hence, we are guaranteed that all the eigenvalues of the matrix $\underline{\mathbf{C}}\,\underline{\mathbf{B}}^{-1}$ are pure imaginary, and the ERK4 scheme is thus appropriate to use.

We now discuss the choice of including the "expansion" term $\underline{\mathbf{E}}^{n+1}\,\underline{\Theta}^{n+1}$ in the outer problem (33). First, this term is derived from the associated bilinear form (9). This bilinear form is symmetric, but has a "coefficient" $\nabla \cdot \mathbf{w}$ which can be either positive or negative definite depending on whether the domain is locally expanding or contracting. The matrix $\underline{\mathbf{E}}$ is therefore symmetric, but the definiteness is not determined. If we include the term $\underline{\mathbf{E}}\,\underline{\Theta}$ in the "inner" problem, the discrete operator in (34) changes from $\underline{\mathbf{C}}\,\underline{\mathbf{B}}^{-1}$ to $(\underline{\mathbf{C}} - \underline{\mathbf{E}})\,\underline{\mathbf{B}}^{-1}$. In this case, we cannot guarantee that all the eigenvalues will remain inside the absolute stability region of ERK4 (or inside the stability region of other explicit time integration schemes) since some eigenvalues may end up with positive real parts.

We remark that the "expansion" term vanishes if we insist on having a divergence free mesh velocity. Such a constraint has been proposed as a way to honor the so-called Geometric Conservation Law (GCL); see [12, 7, 10]. For example, the work presented in [4] honors the GCL condition through the computation of a divergence free mesh velocity, which can be achieved through the solution of a Stokes problem. However, since the significance of the GCL condition is not quite clear for general problems, we will here not assume such a constraint, and we therefore have to treat the additional term appropriately. Our goal with this study is also to gain more insight into the global regularity requirements for the mesh velocity.

From (33) it follows that we need to solve a system of equations for Θ^{n+1} of the form

$$\left(\underline{\mathbf{A}}^{n+1} + \frac{1}{\Delta t}\,\underline{\mathbf{B}}^{n+1} - \underline{\mathbf{E}}^{n+1}\right)\Theta^{n+1} = \underline{\mathrm{b}}^{n+1}, \tag{37}$$

where $\underline{\mathrm{b}}^{n+1}$ represents a known right hand side (we assume that we already have solved the "inner" problem for $\widetilde{\Phi}^{n+1}$). The first two terms inside the parentheses represent the discrete Helmholtz operator. As mentioned earlier, the matrix $\underline{\mathbf{E}}$ is symmetric (and, in our case, diagonal), but we cannot guarantee the definiteness of this matrix. On the other hand, by combining the last two terms inside the parantheses in (37), we conclude that we are guaranteed positive definiteness if

$$(1 - \Delta t \nabla \cdot \mathbf{w}) > 0.$$

However, from the basic definition of the divergence, this is the same as saying that the *relative* change in a small volume element in one single time step should be less than one. This is typically always true: a local volume element will generally not double in size in a single time step. Hence, we can assume that the system matrix in (37) is symmetric and positive definite, and that we can use iterative solvers for such systems, typically, the conjugate gradient method.

The extension to second and third order in time is quite similar to the corresponding extension for fixed domains. For example, a second order splitting scheme will read

$$\left(\frac{\frac{3}{2}\underline{\mathbf{B}}^{n+1}\underline{\Theta}^{n+1} - 2\underline{\widetilde{\Phi}}^{n+1} + \frac{1}{2}\underline{\widetilde{\widetilde{\Phi}}}^{n+1}}{\Delta t}\right) = (-\underline{\mathbf{A}}^{n+1} + \underline{\mathbf{E}}^{n+1})\,\underline{\Theta}^{n+1} + \underline{\mathrm{b}}^{n+1}. \tag{38}$$

where

$$\frac{\mathrm{d}\underline{\widetilde{\Phi}}}{\mathrm{d}t} = -\underline{\mathbf{C}}\,\underline{\mathbf{B}}^{-1}\underline{\widetilde{\Phi}}, \qquad \underline{\widetilde{\Phi}}^{n} = (\underline{\mathbf{B}}\,\underline{\Theta})^{n}, \qquad t^n \le t \le t^{n+1}, \tag{39}$$

$$\frac{\mathrm{d}\underline{\widetilde{\widetilde{\Phi}}}}{\mathrm{d}t} = -\underline{\mathbf{C}}\,\underline{\mathbf{B}}^{-1}\underline{\widetilde{\widetilde{\Phi}}}, \qquad \underline{\widetilde{\widetilde{\Phi}}}^{n-1} = (\underline{\mathbf{B}}\,\underline{\Theta})^{n-1}, \qquad t^{n-1} \le t \le t^{n+1}. \tag{40}$$

In addition, the system (21) is now solved using a second order Adams-Bashforth scheme,

$$\left(\frac{\underline{\mathbf{x}}^{n+1} - \underline{\mathbf{x}}^{n}}{\Delta t}\right) = \frac{3}{2}\,\underline{\mathbf{w}}^{n} - \frac{1}{2}\,\underline{\mathbf{w}}^{n-1}. \tag{41}$$

A special remark is required when solving the "inner" convection problems (39) and (40). For a *fixed* geometry, we recall that we need to use a first order polynomial approximation in time for the convecting velocity field; see Figure 2. For *time-dependent* geometries, we need to use a first order approximation in time for the convecting velocity field, for the mesh velocity, as well as for the geometry. Again, the approximations are based on linear interpolations/extrapolations of the values at t^{n-1} and t^n.

Finally, the approach presented above can readily be extended to a third order splitting scheme. Similar to the fixed geometry case, we need to solve three separate ("inner") convection problems. In addition, the convecting velocity field, the mesh velocity, as well as the geometry are now all constructed as second order interpolants/extrapolants in the interval between t^{n-2} and t^{n+1}. The problem (21) is in this case solved using a third order Adams-Bashforth scheme.

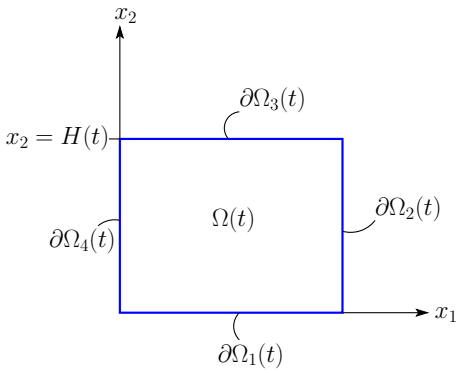

Figure 3: The rectangular domain used for the moving front problem. The height of the domain is given as $H(t)$.

5.3 Numerical results

One difficulty with assessing the accuracy of a discretization scheme in time-dependent domains is the lack of analytical solutions, especially for problems in general domains. We now present a two-dimensional convection-diffusion problem we have designed in order to verify the proposed computational approach in the context of a moving front. Specifically, we consider the solution of the time-dependent convection-diffusion equation

$$\frac{\partial \Theta}{\partial t} + \mathbf{u} \cdot \nabla \Theta = \nabla^2 \Theta + g, \quad \text{in } \Omega(t),$$

where $\Omega(t) = (0,1) \times (0, H(t))$ is the rectangular domain depicted in Figure 3. The boundary conditions are

$$\begin{aligned} \Theta &= 0, \qquad \text{on } \partial\Omega_1(t),\ \partial\Omega_3(t), \\ \frac{\partial \Theta}{\partial n} &= 0, \qquad \text{on } \partial\Omega_2(t),\ \partial\Omega_4(t). \end{aligned}$$

We impose a two-dimensional convecting velocity field $\mathbf{u} = (u_1, u_2)$, with

$$\begin{aligned} u_1(x_1, x_2, t) &= \pi \sin\left(\frac{2\pi x_2}{H(t)}\right) \sin^2(\pi x_1) \sin(t), \\ u_2(x_1, x_2, t) &= -H(t)\pi \sin(2\pi x_1) \sin^2\left(\frac{\pi x_2}{H(t)}\right) \sin(t), \end{aligned}$$

and we choose the right hand side $g(x_1, x_2, t)$ such that the exact solution $\Theta(x_1, x_2, t)$ of the two-dimensional convection-diffusion equation is given as

$$\Theta(x_1, x_2, t) = \sin\left(\frac{\pi x_2}{H(t)}\right).$$

In order to mimic a "melting-front" problem (a Stefan problem), we assume that the speed of the front is determined through the condition

$$\frac{\mathrm{d}H}{\mathrm{d}t} = -\frac{\partial \Theta}{\partial x_2}\bigg|_{x_2 = H(t)}. \tag{42}$$

From the above information we can derive an analytical solution for the front,

$$H(t) = \sqrt{2\pi t + H_0^2}, \tag{43}$$

where H_0 is the "height" of the domain at time $t = 0$.

We first discretize the domain Ω using two spectral elements, Ω_1 and Ω_2. Next, we solve the semi-discrete equations using the splitting method proposed in Section 5.2. Note that we never use our knowledge about the exact solution (43) to advance the front. Instead, we use (42) to compute the x_2-component of the grid velocity, w_2, along the front directly from the numerical solution. This grid velocity is then extended to the interior of the domain by requiring that: (i) the x_1-component of the grid velocity is zero, i.e., $w_1 = 0$ in Ω; (ii) the x_2-component of the grid velocity is extended smoothly from the front to the interior of the domain; specifically, $w_2 \in \mathbb{P}_1(\Omega)$, i.e., w_2 varies linearly with x_2 in Ω.

The linear extension used here can also be regarded as an harmonic extension of the grid velocity along the boundary to the interior of the domain. Such a regular extension of the grid velocity is quite common to use in the context of the ALE-formulation. Another common approach is to use an elasticity solver [14, 8] or a Stokes solver [4].

We now integrate the governing equations until a final time, T, where we compare the numerical solution with the exact solution. The initial and final domain is depicted in Figure 4. Note that we start the simulation with two equal-sized spectral elements and that these will remain equal-sized due to the linearly varying grid velocity in the x_2-direction. In Figure 5 we show the temporal and spatial convergence behavior. The discretization error is measured in the energy-norm by first mapping the solution back to the initial configuration, and then performing the error calculation over $\Omega(t_0)$. When the temporal error is dominating, we clearly see first, second, and third order convergence. When the spatial error is dominating, we obtain exponential convergence until we reach the temporal error level, at which point increasing degree, N, of the polynomial approximation within each spectral element does not have any effect.

Let us now revisit this problem, but this time change the global regularity of the mesh velocity. In particular, let us extend the mesh velocity derived from the numerical solution along the front to the interior of the domain in the following way: As earlier, we set the x_1-component equal to zero, i.e., $w_1 = 0$. However, this time we extend the x_2-component such that $w_2 = 0$ in Ω_1 and $w_2 \in \mathbb{P}_1(\Omega_2)$. Hence, w_2 is very regular within each spectral element (in fact, piecewise linear), but w_2 is globally only $C^0(\Omega)$; see Figure 6. The x_2-component of the grid velocity has a sharp jump in the x_2-derivative along the element boundary. Again, we integrate the equations until a final time T and compare with our earlier results. We limit our comparison to the second order splitting scheme, and when the temporal error is dominating. The convergence results are shown in Figure 7. We observe that it is not necessary to require the ALE mapping to be $C^\infty(\Omega)$, or even $C^1(\Omega)$; in this case, C^0-continuity of the mesh velocity suffices. These results are in agreement with the theoretical analysis and comments given in [9].

6 A convection-Stokes splitting scheme

For the case with a fixed domain, the treatment of (22)-(23) is precisely the OIF-method described in [22]. The extension to time-dependent domains follows a similar approach as for the convection-diffusion equation. The "inner" convection problems are treated similarly to the scalar case. However, we remark that the convection problems now represent nonlinear problems, even in fixed geometries. The "outer" problem can be expressed as

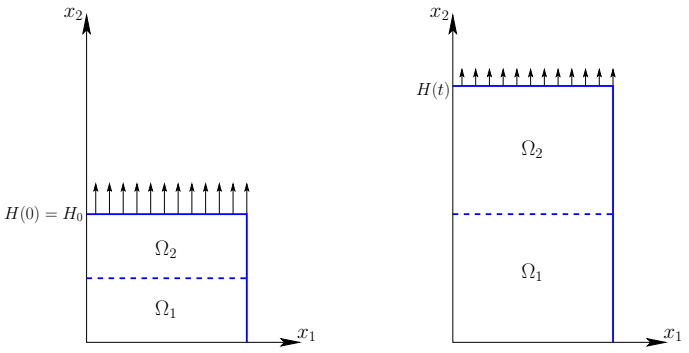

Figure 4: The initial computational domain (left) and the final computational domain (right). The two spectral elements used to solve this problem are denoted as Ω_1 and Ω_2. The mesh velocity computed along the front is extended linearly to zero in the interior of the domain.

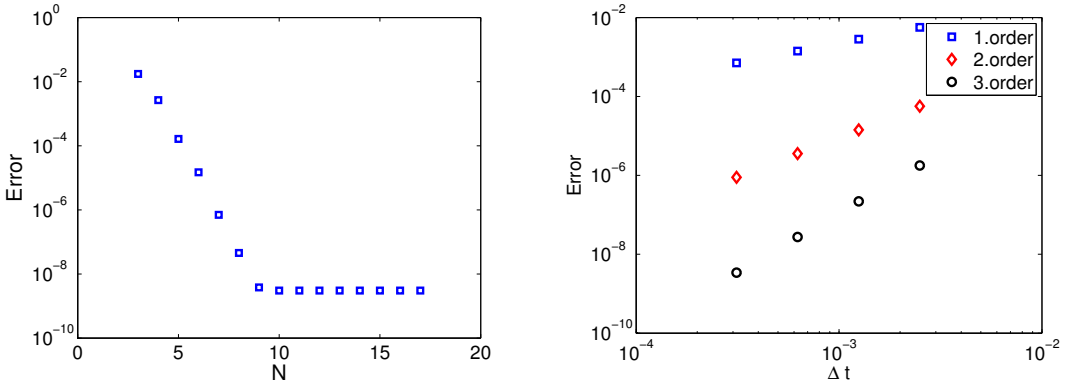

Figure 5: Discretization error in the energy-norm for the moving front test problem. The left plot shows the spatial discretization error as a function of the polynomial degree, N, when the spatial error is dominating. The right plot shows the temporal discretization error as a function of the time step, Δt, when the temporal error is dominating. Results are reported for the first, second, and third order splitting scheme discussed in Section 5.2.

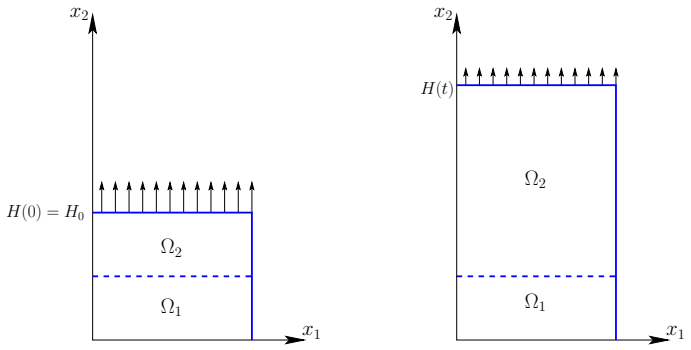

Figure 6: The initial computational domain (left) and the final computational domain (right). The two spectral elements used to solve this problem are denoted as Ω_1 and Ω_2. The mesh velocity computed along the front is here extended linearly to zero in the interior of Ω_2, while the mesh velocity in Ω_1 is identically zero during the entire simulation.

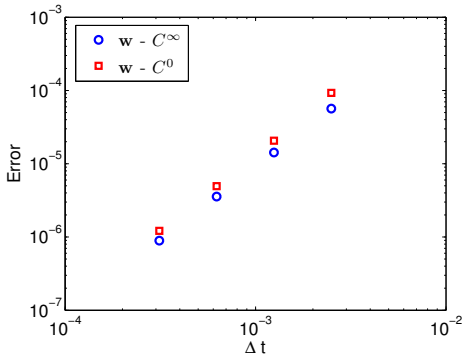

Figure 7: Discretization error in the energy-norm at a final time, T, for the moving front problem. A second order splitting scheme has been used, and the temporal error is dominating. The convergence results using a globally regular mesh velocity (in fact, $w_2 \in C^\infty(\Omega)$) is compared with using a mesh velocity which varies linearly within each spectral element, but is globally only C^0-continuous (with a significant jump in the derivative across the element boundary).

(e.g., for a second order splitting scheme):

$$\left(\frac{\frac{3}{2}\underline{\mathbf{B}}^{n+1}\underline{\mathbf{u}}^{n+1} - 2\underline{\widetilde{\mathbf{\Psi}}}^{n+1} + \frac{1}{2}\underline{\widetilde{\widetilde{\mathbf{\Psi}}}}^{n+1}}{\Delta t} \right) = (-\underline{\mathbf{A}}_{\sigma}^{n+1} + \underline{\mathbf{E}}^{n+1})\,\underline{\mathbf{u}}^{n+1} + \underline{\mathbf{D}}^{T}\underline{p}^{n+1} + \underline{\mathbf{b}}^{n+1}, \quad (44)$$

$$\underline{\mathbf{D}}\,\underline{\mathbf{u}}^{n+1} = 0, \quad (45)$$

where $\underline{\mathbf{\Psi}} = \underline{\mathbf{B}}\,\underline{\mathbf{u}}$ corresponds to the transformation (31) for the convection-diffusion case. The Stokes system (44)-(45) can be solved for the velocity $\underline{\mathbf{u}}^{n+1}$ and $\underline{p}^{n+1}$ via a standard Uzawa decoupling procedure; e.g., see [20]. In the following, we will focus on such a pure convection-Stokes decoupling approach; the alternative is to also include a pressure-velocity decoupling in the Stokes operator.

We remark that the operator splitting scheme presented here, i.e., the convection-Stokes splitting scheme for the semi-discrete Navier-Stokes equations, or the convection-diffusion splitting scheme presented in the previous section, will include temporal splitting errors at steady state (for problems where a steady state solution exists). This is similar to the OIF-method applied to problems in fixed geometries. The reason for this can be understood by interpreting the splitting scheme as a semi-Lagrangian scheme were the total derivative is approximated along the characteristics in the upwind direction via a first, second, or third order backward differentiation scheme. In particular, the left-hand side of (38) and the left hand side of (44) both represent a streamline-upwind approximation to the convective term.

Note also that, similar to the convection-Stokes splitting presented in [22] for fixed geometries, no interpolation between the grid points is needed in order to determine the necessary field values along the characteristics; the solution of the "inner" convection subproblems will give us the necessary information only using values at the current and previous time steps, and only using the nodal values (i.e., the values at the grid points) at the current and previous time steps.

6.1 Numerical results

We now verify our discretization approach by solving the three-dimensional Navier-Stokes equations in a cube. The domain boundary is fixed at all times, however, we specify an artificial time-periodic mesh velocity in the interior. The mesh velocity is a function of both space (all the coordinates) and time, and is zero on the domain boundary. We also specify a forcing function in the momentum equations by requiring that the following analytic solution satisfies the incompressible Navier-Stokes equations:

$$u_1(x_1, x_2, x_3, t) = \frac{\pi}{5}\sin^2(\pi x_1)\sin(2\pi x_2)\sin(2\pi x_3)\sin(t), \quad (46)$$

$$u_2(x_1, x_2, x_3, t) = -\frac{\pi}{10}\sin(2\pi x_1)\sin^2(\pi x_2)\sin(2\pi x_3)\sin(t), \quad (47)$$

$$u_3(x_1, x_2, x_3, t) = -\frac{\pi}{10}\sin(2\pi x_1)\sin(2\pi x_2)\sin^2(\pi x_3)\sin(t), \quad (48)$$

$$p(x_1, x_2, x_3, t) = \cos(\pi x_1)\sin(\pi x_2)\sin(\pi x_3)\sin(t). \quad (49)$$

Note that the prescribed mesh velocity is only C^0-continuous in space. Inside each spectral element, the mesh velocity is analytic in both space and time. However, the gradient of the mesh velocity is not continuous across element boundaries; in fact, the mesh velocity is identically zero in one of the spectral elements. On the other hand, we impose a mesh velocity which is very regular in time; see Figure 8. Finally, we remark that the mesh velocity is not divergence free. The convergence results in Figure 9 show the

anticipated behavior: first, second, and third order convergence in time, and exponential convergence in space for problems with analytic solutions and data.

Even though we are using isoparametric spectral elements, the geometry representation is in this case effectively built upon using a trilinear approximation within each element; this is due to the fact that all element edges (internal and external) are straight. The mesh velocity is here constructed in the following way: we first define some non-trivial motion of the internal element *vertices*. We then define the mesh velocity in such a way that a numerical integration of (24) using Adams-Bashforth methods results in straight spectral element edges. One reason for doing this is to ensure a perfect distribution of all the spectral element nodes during the simulation.

The test reported here is obviously a very artificial one; the natural choice is to use a fixed geometry since the external boundary of the cube is fixed. However, aside from providing information about the discretization error using the ALE formulation and a splitting approach, this test also allows us to repeat the numerical experiment using a fixed geometry and compare the discretization errors. In Figure 10 we compare the temporal and spatial errors when using a fixed geometry (i.e., $\mathbf{w} = \mathbf{0}$), and when imposing the artificial mesh velocity depicted in Figure 8. For example, for a fixed Δt, this plot indicates "the price" we have to pay for using an ALE-formulation where we could have expressed the governing equations in a fixed geometry. For the particular test problem we have chosen here, our numerical results indicate that this "price" is about one order or magnitude for a second order scheme and about two orders of magnitude for a third order scheme.

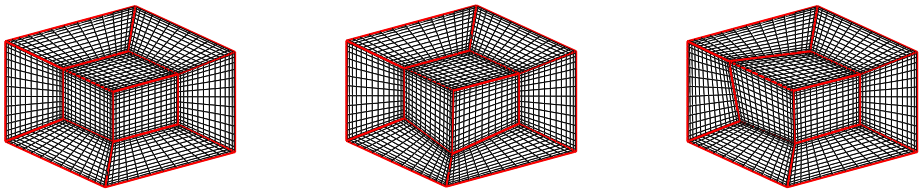

(a) $t = 0$ (b) $t = 0.2$ (c) $t = 0.4$

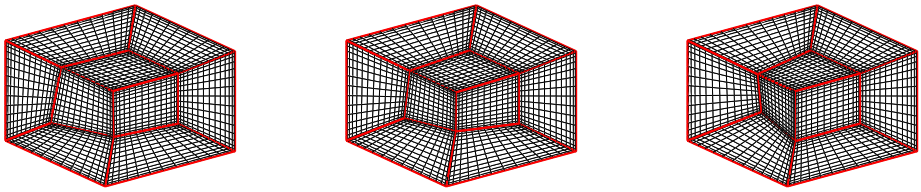

(d) $t = 0.6$ (e) $t = 0.8$ (f) $t = 1.0$

Figure 8: The three-dimensional box used in the convergence study of the ALE scheme. The domain is decomposed into seven spectral elements, one in the middle of the domain and one connected to each of the six faces of the box. The external boundary of the box is fixed. However, we specify a mesh velocity in the interior of the cube which is a function of both space and time (periodic in time). The plot indicates the grid-configuration at a few time levels for five of the spectral elements during one single period. The exact flow solution in the domain is given by (46)-(49).

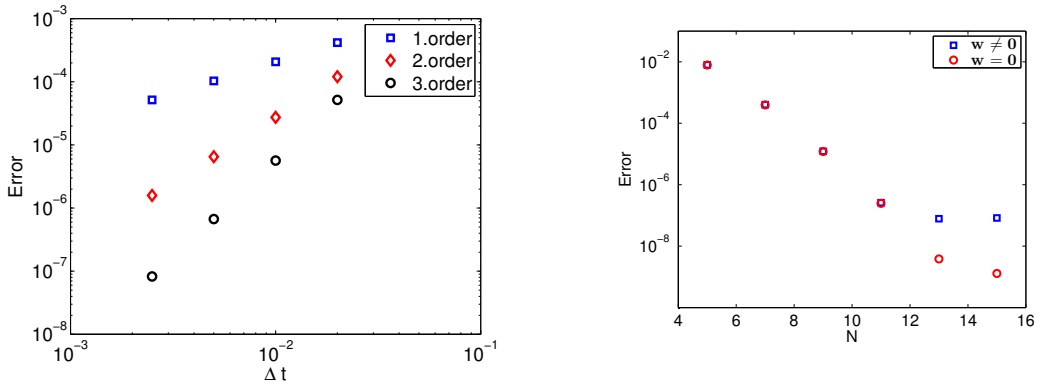

Figure 9: The left plot depicts the discretization error in the energy norm at time $T = 3$ as a function of the time step, Δt, for a first, second, and third order temporal splitting scheme; the spatial error is here subdominant the temporal error. The right plot depicts the discretization error as a function of the polynomial degree, N, used in each spectral element; the temporal error is here subdominant the spatial error for $N < 12$.

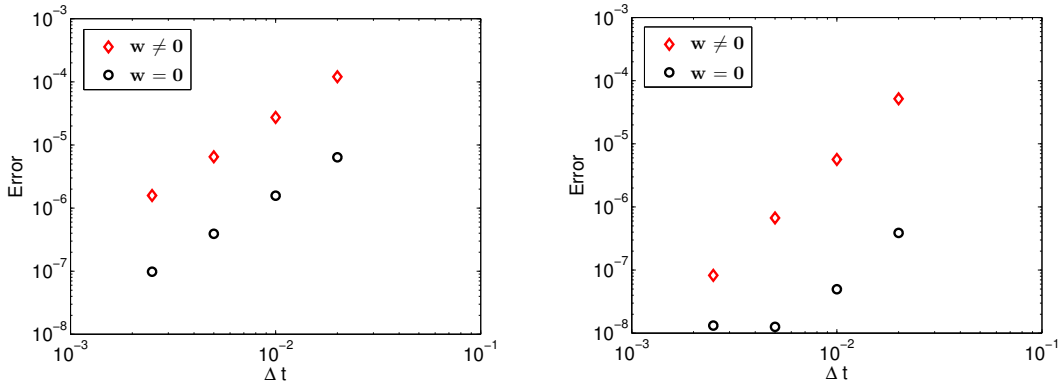

Figure 10: A comparison of the discretization error in the energy norm at time $T = 3$ with and without imposing an artificial mesh velocity in the interior of the domain; see Figure 8. The left plot shows the temporal error for the second order OIF splitting scheme, while the right plot shows the corresponding results for a third order scheme. The spatial discretization error is here on the order of 10^{-8}.

6.2 Comparison with other schemes

We now compare the OIF splitting approach for the convection-Stokes splitting with two other schemes: the scheme discussed in [14] (the HP scheme), and a slightly modified version of the scheme discussed in [17] (the KIO scheme) and used for moving boundary problems in [4]. The difference between the KIO scheme and the scheme used in this work is that we do not split the Stokes operator into a separate pressure step and a separate viscous step.

Similar to the OIF-scheme, both these schemes treat the convection term explicitly, while the Stokes operator is treated implicitly using a backward difference scheme. With reference to the semi-discrete equations (24), these two schemes can be expressed succinctly as

$$\frac{1}{\Delta t}\sum_{k=0}^{s}\beta_k(\underline{\mathbf{B}}\,\underline{\mathbf{u}})^{n+1-k} = -(\underline{\mathbf{A}}_\sigma\,\underline{\mathbf{u}})^{n+1} + (\underline{\mathbf{D}}^T\underline{p})^{n+1} + \sum_{k=0}^{s}\alpha_k((\underline{\mathbf{C}}+\underline{\mathbf{E}})\underline{\mathbf{u}})^{n-k} + \underline{\mathbf{b}}^{n+1}. \quad (50)$$

Here, s is the order of the scheme. The treatment of the divergence constraint and the mesh evolution is similar to the OIF-scheme.

In [14], α_k, $k = 0, 1, 2$, where chosen to be modified AB-coefficients for a second order scheme, while in [17], α_k, $k = 0, 1$, were chosen such that they correspond to a linear extrapolation of the convection term at time t^{n+1}. In Table 1 we also give the corresponding coefficients for a third order approach.

In Figure 11 we report numerical results showing a comparison of the three methods. We see that all methods give the correct order, and also give very similar results (with the OIF scheme proposed in this work giving a marginally better constant).

		First order	Second order	Third order
BD	β_0	1	$\frac{3}{2}$	$\frac{11}{6}$
	β_1	-1	-2	-3
	β_2	0	$\frac{1}{2}$	$\frac{3}{2}$
	β_3	0	0	$-\frac{1}{3}$
HP	α_0		$\frac{8}{3}$	$\frac{15}{4}$
	α_1		$-\frac{7}{3}$	$-\frac{21}{4}$
	α_2		$\frac{2}{3}$	$\frac{13}{4}$
	α_3		0	$-\frac{3}{4}$
KIO	α_0		2	3
	α_1		-1	-3
	α_2		0	1
	α_3		0	0

Table 1: Backward Differentiation (BD) coefficients β_k, together with the coefficients α_k; see (50). The coefficients α_k for the HP scheme are taken from [14] (second order scheme only), while the coefficients for the KIO scheme are taken from [17].

7 Conclusions

We have presented a temporal splitting scheme for the semi-discrete convection-diffusion equation and the semi-discrete incompressible Navier-Stokes equations in time-dependent

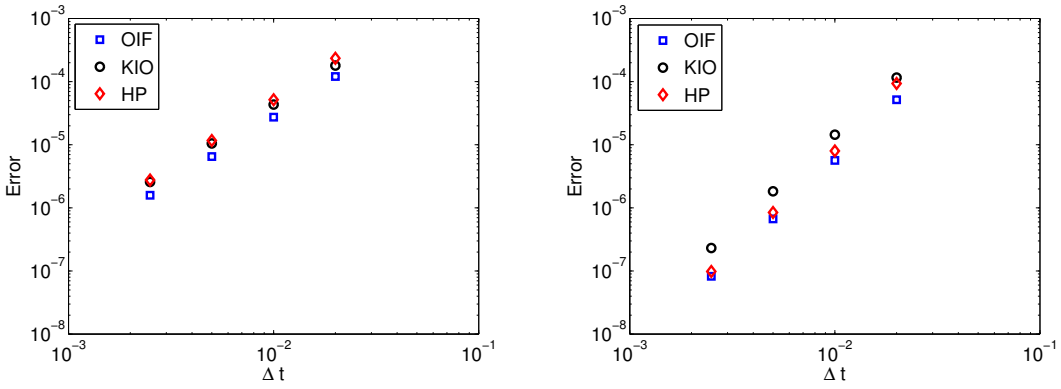

Figure 11: A comparison of the temporal error in the energy norm as a function of the time step, Δt, for the following second order (left plot) and third order (right plot) schemes: the OIF scheme presented in this paper, the HP splitting scheme discussed in [14] (also extended to third order in this study), and the KIO splitting scheme discussed in [17] (here used in a slightly modified form). For all these results, the spatial error is subdominant the temporal error.

domains. The proposed splitting scheme can be considered as an extension of the OIF-method proposed in [22] in the sense that it can be interpreted as a semi-Lagrangian method for time-dependent domains. The computational approach has been tested numerically on model problems with known analytical solutions, for which first, second, and third order convergence has been obtained. Based on the experience so far, the results for the OIF splitting scheme compares favorably with two alternative approaches proposed in the literature. The approach has been used successfully in the context of simulating three-dimensional Bénard-Marangoni flows with a deformable free surface [3].

We remark that all the splitting schemes discussed in this paper for the Navier-Stokes equations fundamentally focus on two types of splittings: (i) splitting the treatment of the geometry evolution from the treatment of the interior Navier-Stokes calculation; and (ii) splitting the treatment of the (ALE) convection operator in the fluid problem from the Stokes operator. We have not considered splitting the Stokes operator itself into a pressure step and a viscous step; this would have introduced an additional splitting error. Instead, we have solved the unsteady Stokes problem via a standard Uzawa algorithm, which does not correspond to a rediscretization of the Stokes operator, but rather a decoupling algorithm.

The numerical results show that the mesh velocity introduced in the ALE-formulation does not have to be globally smooth in space. In the context of the isoparametric spectral element discretization used in this study, it is sufficient that the mesh velocity is regular within each spectral element, and C^0-continuous across element boundaries. Hence, the extension of the mesh velocity from the boundary to the interior does not necessarily have to be obtained through the use of an elliptic solver which is commonly the case. This observation is consistent with the theoretical discussion and comments in [9]. This could allow for the use of faster and more flexible ways of updating the mesh velocity at each time step; we plan to explore this opportunity in a future study. Note that, in order to obtain high order temporal accuracy, the mesh velocity should be regular in the time direction.

The proposed splitting method does not appear to satisfy the Geometric Conservation Law. Based on the tests we have done so far, we have thus not been able to conclude to what

extent the quality of a general Navier-Stokes solution will improve if the GCL condition is satisfied. We remark that the mesh velocity used in this study is not divergence free.

Despite the encouraging results obtained in this study, more quantitative comparisons still need to be done in the context of free surface problems with larger and more complex deformations (i.e., free surfaces with significant curvature). An obvious challenge is to derive analytical solutions in more complex time-dependent domains. However, we believe it is necessary to obtain quantitative results for more complex problems in order to discriminate the quality of different ALE-solvers used in a more realistic setting. For example, controlling the accuracy of a moving interface with a varying (mean) curvature is a non-trivial task which we feel has not yet been treated satisfactorily in the literature; the interface-tracking issue is currently under investigation in a separate study.

Acknowledgment

The authors would like to thank the Norwegian University of Science and Technology for the financial support of this project.

References

[1] R. Aris. *Vectors, Tensors, and the Basic Equations of Fluid Mechanics*. Dover Publications, Inc., 1962.

[2] T. Bjøntegaard and E.M. Rønquist. High order methods for incompressible fluid flow: Application to free surface problems. In B. Skallerud and H. I. Andersson, editors, *MekIT'07*. Tapir Akademisk Forlag, 2007.

[3] T. Bjøntegaard and E.M. Rønquist. Simulation of three-dimensional Bénard-Marangoni flows including deformed surfaces. *Communications in Computational Physics*, to appear.

[4] N. Bodard, R. Bouffanais, and M.O. Deville. Solution of moving-boundary problems by the spectral element method. *Applied Numerical Mathematics (2007),doi:10.1016/j.apnum.2007.04.009*, 2007.

[5] D. Boffi and L. Gastaldi. Stability and geometric conservation laws for ALE formulations. *Computer Methods in Applied Mechanics and Engineering*, 193:4717–4739, 2004.

[6] J. Donea S. Giuliani and J.P Halleux. An arbitrary Lagrangian-Eulerian finite element method for transient dynamic fluid-structure interactions. *Computer Methods in Applied Mechanics and Engineering*, 33:689–723, 1982.

[7] C. Farhat and P. Geuzaine. Design and analysis of robust ALE time-integrators for the solution of unsteady flow problems on moving grids. *Computer Methods in Applied Mechanics and Engineering*, 193:4073–4095, 2004.

[8] C. Farhat, M. Lesoinne, and N. Maman. Mixed explicit/implicit time integration of coupled aeroelastic problems: three-field formulation, geometry conservation and distributed solution. *International Journal for Numerical Methods in Fluids*, 21:807–835, 1995.

[9] L. Formaggia and F. Nobile. A stability analysis for the arbitrary Lagrangian Eulerian formulation with finite elements. *East-West Journal of Numerical Mathematics*, 7(2):105–131, 1999.

[10] L. Formaggia and F. Nobile. Stability analysis of second-order time accurate schemes for ALE-FEM. *Computer Methods in Applied Mechanics and Engineering*, 193:4097–4116, 2004.

[11] F.X. Giraldo. The Lagrange-Galerkin Spectral Element Method on Unstructured Quadrilateral Grids. *Journal of Computational Physics*, 147:114–146, 1998.

[12] H. Guillard and C. Farhat. On the significance of the geometric conservation law for flow computations on moving meshes. *Computer Methods in Applied Mechanics and Engineering*, 190:1467–1482, 2000.

[13] C.W. Hirt, A.A. Amsden, and J.L Cook. An arbitrary Lagrangian-Eulerian computing method for all flow speeds. *Journal of Computational Physics*, 14:227–253, 1974.

[14] L.W. Ho and A.T. Patera. A Legendre spectral element method for simulation of unsteady incompressible viscous free-surface flows. *Computer Methods in Applied Mechanics and Engineering*, 80:355–366, 1990.

[15] A. Huerta and A. Rodríguez-Ferran (eds.). The Arbitrary Lagrangian-Eulerian Formulation. *Computer Methods in Applied Mechanics and Engineering*, 193(39-41):4073–4456, 2004.

[16] T.J.R. Hughes, W.K. Liu, and T.K Zimmermann. Lagrangian-Eulerian finite element formulation for incompressible viscous flows. *Computer Methods in Applied Mechanics and Engineering*, 29:329–349, 1981.

[17] G.E. Karniadakis, M. Israeli, and S.A. Orszag. High-Order Splitting Methods for the Incompressible Navier-Stokes Equations. *Journal of Computational Physics*, 97:414–443, 1991.

[18] M. Lesoinne and C. Farhat. Geometric conservation laws for flow problems with moving boundaries and deformable meshes, and their impact on aeroelastic computations. *Computer Methods in Applied Mechanics and Engineering*, 134:71–90, 1996.

[19] G. Løland and J.V. Aarsnes. Fabric as construction material for marine applications. *Hydroelasticity in Marine Technology*, pages 275–286, 1994.

[20] Y. Maday, D. Meiron, A.T. Patera, and E.M. Rønquist. Analysis of iterative methods for the steady and unsteady stokes problem: application to spectral element discretizations. *SIAM Journal on Scientific Computing*, 14(2):310–337, 1993.

[21] Y. Maday and A.T. Patera. Spectral element methods for the Navier-Stokes equations. *in: A.K. Noor, J. T. Oden (Eds.), State of the Art Surveys in Computational Mechanics, ASME, New York*, pages 71–143, 1989.

[22] Y. Maday, A.T. Patera, and E.M. Rønquist. An Operator-Integration-Factor Splitting Method for Time-Dependent Problems: Application to Incompressible Fluid Flow. *Journal of Scientific Computing*, 5(4):263–292, 1990.

[23] D. Xiu and G.E. Karniadakis. A Semi-Lagrangian High-Order Method for Navier-Stokes Equations. *Journal of Computational Physics*, 172:658–684, 2001.